Activitas Nervosa Superior Rediviva Volume 64 No. 1 2022

ORIGINAL ARTICLE

Evaluation of Brain Connectivity Alteration in Patients with Knee Osteoarthritis, Using Matrix-Variate Differential Network Model

Fatemeh Pourmotahari [1], Nasrin Borumandnia [2], Seyyed Mohammad Tabatabaei [3,4], Naghmeh Khadembashi [5], Hamid Alavimajd [1]

[1] Department of Biostatistics, Faculty of Paramedical Sciences, Shahid Beheshti University of Medical Sciences, Tehran, Iran, [2] Urology and Nephrology Research Center, Shahid Beheshti University of Medical Sciences, Tehran, Iran, [3] Department of Medical Informatics, Faculty of Medicine, Mashhad University of Medical Sciences, Mashhad, Iran, [4] Clinical Research Development Unit, Imam Reza Hospital, Mashhad University of Medical Sciences, Mashhad, Iran, [5] English Language Department, School of Allied Medical Sciences, Shahid Beheshti University of Medical Sciences, Tehran, Iran.

Correspondence to: Alavimajd H, Department of Biostatistics, Faculty of Paramedical Sciences, Shahid Beheshti University of Medical Sciences, Qods Square, Tajrish, Tehran, Iran
TEL: +982122707347; E-MAIL: alavimajd@sbmu.ac.ir

Submitted: 2022-03-15 Accepted: 2022-04-19 Published online: 2022-04-19

Key words: **chronic pain; knee osteoarthritis; functional brain imaging; fMRI; graphical model**

Act Nerv Super Rediviva 2022; **64**(1): 18–24 ANSR64122A04

Abstract

OBJECTIVES: Knee osteoarthritis (KOA) is a common disease that causes chronic pain, affecting the quality of life. However, the neural mechanisms of pain in osteoarthritis of the knee are not fully understood. Brain connectivity studies can provide information about the exact mechanism of the disease to manage pain by examining patterns among the different regions of the brain. The present study aimed to determine functional relationship changes in KOA patients using an advanced statistical method.

METHODS: Resting-State functional MRI imaging information was downloaded from the "openneuro" site. These data are related to 12 healthy individuals with a mean age of 58.75 and 36 KOA patients with a mean age of 57.58. In this study, a matrix-variate statistical model was used to determine changes in communication patterns among different brain regions in KOA patients.

RESULTS: The functional connectivity results of 42 different edges between the patient and healthy groups showed that in more than half of them, the connectivity in the patient group was reduced compared to healthy individuals. Heschl's and middle temporal areas had a greater reduction of communication compared to other areas. Also, in a part of the default mode network, functional connectivity alteration with left caudate, left putamen, left thalamus, and lingual right areas were observed.

CONCLUSIONS: This study showed a change in functional communication patterns in patients with KOA, which could indicate the effect of chronic pain on changes in brain function and cognitive processes.

Introduction

Chronic pain (CP) is one of the most common and complex public health problems that cause persistent unpleasant physical and mental conditions. The average prevalence of chronic pain in each country is reported to be between 18% to 40%, and the resulting burden is increasing worldwide (Elzahaf *et al.* 2012; Jackson *et al.* 2016; Sá *et al.* 2019). Since pain is a subjective feeling, its objective measurement is associated with problems; so, due to the high cost of health care, the assessment of chronic pain management in patients is not done well (Galer & Jensen 1997; Edwards *et al.* 2016).

Knee osteoarthritis (KOA) is the most common cause of chronic pain that affects a person's quality of life. KOA is a multi-factorial disease that progresses slowly and mostly affects knee joints. The most crucial symptom in diagnosing knee osteoarthritis is persistent pain, which is associated with decreased physical function and muscle weakness. Several treatments are often related to symptom relief, and despite recent advances in the pathogenesis of the disease, there exists no treatment that reduces symptoms and prevents disease progression. Therefore, using appropriate measurement tools to identify the exact mechanisms of the disease can improve pain management (Felson 2009; Michael *et al.* 2010; Schaible 2012; Lu *et al.* 2015; Lespasio *et al.* 2017; Lambova & Müller-Ladner 2018).

Functional magnetic resonance imaging (fMRI) is a powerful non-invasive tool that can provide information on brain mechanisms of pain. In this method, blood-oxygen-level- dependent (BOLD) signals of active areas of the brain, are measured. Then the functional connectivity (FC) method recognizes the variation of brain communication patterns between healthy and sick people by estimating the temporal correlation of these signals. FC studies are used in various clinical areas, including patients with chronic pain (Brodersen *et al.* 2012; Tanasescu *et al.* 2016; Cottam *et al.* 2018). In this regard, several studies have reported changes in the functional relationship of the default mode network (DMN) in patients with chronic pain (Napadow *et al.* 2010; Loggia *et al.* 2013; Baliki *et al.* 2014; Hemington *et al.* 2016). However, there are contradictions regarding the increase or decrease of communication in this network, which can be related to the type of statistical model used.

Analysis of brain connectivity patterns is usually based on graph theory techniques. In these methods, the brain network is shown in the form of a graph in which the desired brain areas are nodes, and the correlation between them is shown as the edge. The correlation coefficient between areas of the brain (for example, Pearson correlation coefficient, mutual information, and partial correlation coefficient) is calculated to estimate the edges; then, the hypothesis of equality of FC patterns between the healthy and sick groups is calculated (Sporns *et al.* 2000; Bullmore & Sporns 2009; Zalesky *et al.* 2010; Smith *et al.* 2011). However, in FC analysis models, most data forms are considered linear vector distributions based on regions, ignoring the dependence between the values of time series, which may lead to incorrect results. Therefore, in this study, an advanced statistical model has been used which, considering the D-trace loss function and Lasso-type penalty, identifies the differences in FC patterns of KOA patients compared to healthy individuals (Ji *et al.* 2020).

Materials and methods

Subject

This study examined resting-State fMRI data of thirty-six KOA patients (45-70 years old; 18 females and 18 males) and twelve healthy individuals (48-78 years old; 5 females and 7 males). There was no significant difference in age (p-value = 0.567) and sex (p-value = 0.617) distribution between the two groups.

Data acquisition

The data of this study was downloaded from the openneuro.org database with document ID "ds000208". Information about taking fMRI images: The scans acquisition protocol was obtained as follows: TR = 2.5 s, TE = 30 ms, thickness=3 mm, matrix size=64 × 64, flip angle = 90, the number of volumes was 300.

Data processing

Pre-processing of resting-state fMRI scans was performed using FSL software version 6.0.1. The first 10 volumes of each time course were removed due to the correction of the initial image inhomogeneity and the adaptation of people to the surrounding conditions. A total of 290 values per person was considered. Images were normalized with a voxel resolution of 2 * 2 * 2 mm3 and were smoothed using a Gaussian filter with 6 mm FWHM. Then, the pre-processed images were divided into 90 regions of interest (ROIs) according to the AAl atlas by WFU Pickatlas toolbox in MATLAB R2019b software (Tzourio-Mazoyer *et al.* 2002). By removing the regions whose time series showed zero, 70 ROIs were considered to be examined in this study.

Statistical analysis

The brain connectivity of KOA patients was compared to the healthy group based on the matrix-variate differential network (MVDN) model. An essential feature of this model is the ability to consider the matrix structure of fMRI data so that the rows present the ROIs and columns show the time series of the BOLD values.

Let's assume that the spatial-temporal matrices X and Y for the healthy and diseased groups have a matrix normal distribution with the Kronecker product covariance structure, respectively:

$$X \sim N_{p,q}(0_{p,q}, \sum_{T_X} \otimes \sum_{S_X})$$

$$Y \sim N_{p,q}(0_{p,q}, \sum_{T_Y} \otimes \sum_{S_Y})$$

$$\Omega_{S_X} = \sum_{S_X}^{-1}, \quad R_{S_X} = D_{S_X}^{1/2} \Omega_X D_{S_X}^{1/2}$$

$$\Omega_{S_Y} = \sum_{S_Y}^{-1}, \quad R_{S_Y} = D_{S_Y}^{1/2} \Omega_Y D_{S_Y}^{1/2}$$

p represents the number of desired regions, and q represents the number of time series of BOLD values. The R_{SX} and R_{SY} are the partial correlation matrices of the patient and the healthy groups, respectively. D_S is the diagonal matrix of Ω_S^{-1}. $\Sigma_{TX}$and Σ_{TY} are considered nuisance parameters. Next, the difference between the estimates of the spatial partial correlation matrix of the two groups $\Delta = R_{SY} - R_{SX}$ is calculated using the D- trace loss function and Lasso-type penalty for identifying functional communication networks between the patient and healthy groups. The interpretation of the FC between brain regions is based on the estimation of the Δ matrix, so that non-zero values in this matrix show a significant difference in the correlation of brain regions between the two groups, and zero values indicate no difference (Ji *et al.* 2020).

Results

The difference in brain communication patterns between the two groups of KOA patients and healthy individuals was estimated by the MVDN model. Figure 1 shows the different edges of the brain network between the patient and healthy groups in three forms: axial view, coronal view, and sagittal view. In this diagram, the increase of functional relationship of the healthy group compared to KOA patients is manifested with a green edge, and the decrease of functional relationship is manifested with a yellow edge. A total of 42 different edges were identified between the study groups, about 60% of which had reduced functional association of patients' brain areas compared to healthy individuals.

In patients, the degree of dependence of the central brain regions with the left medial frontal, left inferior frontal (orbital part), and left middle temporal areas were less, and with the right caudate, right thalamus, and right Heschl areas were more. Functional relationship of the following regions in control group compared to patient group was more: left Heschl - right middle frontal, left supplementary motor, right caudate, left pallidum as well as middle temporal - right inferior frontal (triangular part), left Rolandic, right olfactory, left superior temporal.

Moreover, there were visible functional alterations in part of the default mode network between the two groups. For example, in the patient group, the connection of the cingulum area (anterior and posterior) with

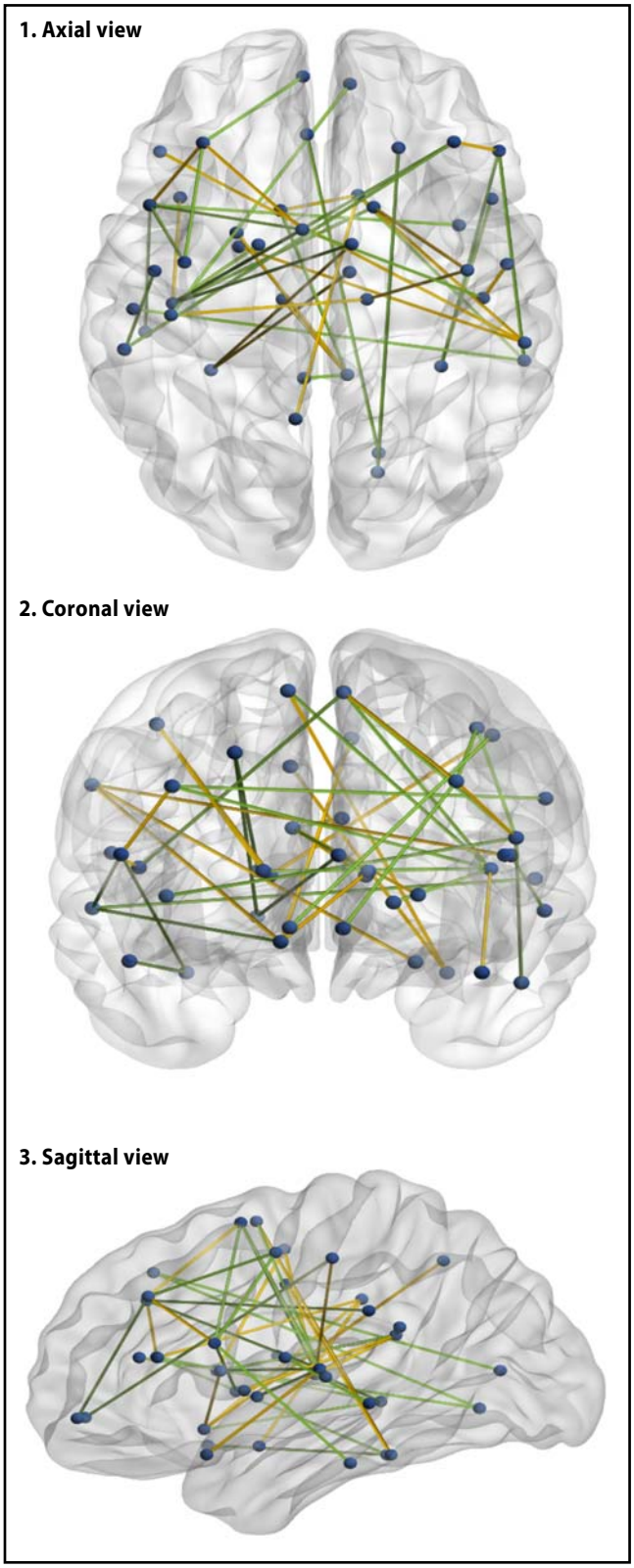

Fig. 1. Differentially expressed edges by MVDN method: green edges show an increase in partial correlation between areas of the brain of healthy individuals compared to the patient group, and yellow edges show a decrease in correlation.

Tab. 1. Differentially expressed edges between brain areas; the ⇑ symbol shows an increase in the correlation between brain areas in healthy individuals compared to KOA patients. The ⇓ symbol shows the decrease in this correlation.

	Different expressed edges			KOA*	Control*	Increase/decrease
1	PreCG.L	⟺	MFG.L	-0.762	0.620	⇑
2	PreCG.L	⟺	IFGoperc.L	-0.675	0.348	⇑
3	MFG.L	⟺	IFGoperc.L	0.299	0.425	⇓
4	MFG.R	⟺	IFGtriang.R	0.237	0.276	⇓
5	MFG.L	⟺	SMA.L	-0.404	0.685	⇓
6	IFGoperc.L	⟺	SMA.L	-0.888	-0.143	⇑
7	MFG.L	⟺	ORBsupmed.L	0.724	-0.505	⇑
8	IFGoperc.L	⟺	INS.R	0.713	-0.100	⇑
9	PCG.L	⟺	PCG.R	0.933	0.921	⇑
10	SFGdor.R	⟺	CAL.R	0.753	0.052	⇑
11	SFGdor.R	⟺	LING.R	0.685	-0.165	⇑
12	ACG.L	⟺	LING.R	-0.522	0.155	⇑
13	SMA.R	⟺	FFG.L	-0.259	-0.868	⇓
14	DCG.R	⟺	FFG.L	-0.104	-0.702	⇓
15	IFGtriang.R	⟺	FFG.R	0.771	0.295	⇑
16	ORBsupmed.R	⟺	PoCG.L	-0.699	-0.573	⇑
17	MFG.R	⟺	SMG.L	-0.302	0.205	⇑
18	IFGtriang.L	⟺	SMG.R	-0.547	-0.766	⇓
19	OLF.R	⟺	SMG.R	-0.336	-0.521	⇓
20	AMYG.L	⟺	SMG.R	-0.265	-0.561	⇓
21	OLF.R	⟺	PCUN.L	-0.500	-0.624	⇓
22	OLF.R	⟺	CAU.L	0.646	0.716	⇓
23	PCG.R	⟺	CAU.L	-0.652	-0.515	⇑
24	PreCG.R	⟺	CAU.R	-0.710	-0.839	⇓
25	PCG.R	⟺	PUT.L	-0.451	-0.483	⇓
26	PCG.R	⟺	THA.L	-0.612	-0.708	⇓
27	PreCG.R	⟺	THA.R	-0.609	-0.802	⇓
28	PoCG.L	⟺	THA.R	-0.572	-0.606	⇓
29	MFG.R	⟺	HES.L	0.349	-0.251	⇑
30	SMA.L	⟺	HES.L	0.495	-0.210	⇑
31	SMA.R	⟺	HES.L	0.538	-0.171	⇑
32	CAU.R	⟺	HES.L	-0.586	0.148	⇑
33	PAL.L	⟺	HES.L	-0.610	0.254	⇑
34	ROL.R	⟺	HES.R	0.944	0.964	⇓
35	SMA.L	⟺	HES.R	0.774	-0.002	⇑
36	HES.L	⟺	TPOsup.L	-0.236	0.494	⇓
37	FFG.R	⟺	TPOsup.R	0.920	0.871	⇑
38	ROL.L	⟺	MTG.L	0.611	0.461	⇑
39	IFGtriang.R	⟺	MTG.R	0.759	0.416	⇑
40	OLF.R	⟺	MTG.R	0.412	0.170	⇑
41	STG.L	⟺	MTG.R	-0.081	0.006	⇑
42	IFGoperc.L	⟺	ITG.L	0.830	0.289	⇑

* Partial correlation values between regions in KOA patient group and control group.
Further details on the full names of the target areas (ROIs) are available in the appendix.

the left caudate and right lingual areas decreased; on the other hand, the connection of the left precuneus area with the right olfactory area increased. Further details of the extent of correlation changes between brain regions are shown in table 1.

Discussion

This study investigated functional alterations (FC alterations) of KOA patients using the MVDN method. Since the structure of fMRI data is defined based on the time series characteristics of BOLD values in each region of the brain, it seems appropriate to use this model, which uses the matrix structure of the data according to their form. In this model, the rows present the different areas of the brain, and the columns show the time series of the areas. Previous models of differential networks often consider the data form as a linear vector distribution based on regions. In these cases, ignoring the dependence between BOLD values at different times may lead to incorrect results. The model used in this study, assuming the matrix-normal distribution for fMRI data and considering the D-trace loss function and Lasso-type penalty, aims at identifying the functional communication patterns in KOA patients.

According to the result of this model, in patients, the functional relationship in more than half of the edges was less than healthy individuals. Heschl and middle temporal regions had a greater decrease in communication compared to the other regions. In this regard, Selvarajah *et al.* (2018) reported a reduction in the functional association of the postcentral, superior frontal, and Heschl areas in patients with painful diabetic neuropathy. This study showed that chronic pain has a significant effect on brain function in diabetic patients. The results of another study on patients with chronic musculoskeletal pain showed a significant difference in Heschl's neural activity between the patient and healthy groups (Taylor *et al.* 2016). Heschl's gyrus is an area of the primary auditory cortex involved in memory, learning, and emotional processing (Da Costa *et al.* 2011; Weinberger 2015; Concina *et al.* 2019). The middle temporal gyrus is also involved in the processes such as language and semantic memory processing (Onitsuka *et al.* 2004) .Hence, functional changes in these areas in patients with chronic pain can disrupt cognitive processes. On the other hand, the present study showed an increase in the dependence of the left amygdala - right supramarginal areas in KOA patients compared to healthy individuals, which is in line with the study of Timmers *et al.* (2021), which was performed on young people with chronic pain. The dependence of right insula- left inferior frontal (opercular part) areas in the patient group was reduced. In this regard, the results of another study on KOA patients showed that the degree of negative correlation between right insula and DMN has increased (Cottam *et al.* 2018).

DMN is one of the main networks whose function changes under the influence of chronic pain. These functional changes can have a great impact on cognitive processes (Alshelh *et al.* 2018). This study examined the frontal superior medial, cingulum (anterior and posterior), and precuneus areas as key parts of this network. The functional alteration of this network with the right olfactory, left caudate, left putamen and left thalamus, and right lingual were observed. In this regard, Lan *et al.* (2020) reported an increase in functional association between the left precuneus gyrus and right supplementary motor areas of the patients compared to the control group through examining the functional changes in the brains of KOA patients older than 65. In addition, several studies have shown functional changes in DMN areas in patients with chronic pain(Baliki *et al.* 2008; Kucyi *et al.* 2014; Alshelh *et al.* 2018; Čeko *et al.* 2020).

Conclusion

This study investigated changes in brain connectivity in patients with KOA using an advanced matrix-variate model. The finding showed different dependencies between the brain areas of the patient group and healthy individuals, which could indicate the effect of chronic pain on changes in overall brain function and impaired cognitive processes.

Acknowledgments

We would thank the openneuro team for sharing the imaging data.

Competing interests

Authors state no conflict of interest.

Ethical approval

Ethical approval was waived for this study, due to the data of this study were downloaded from the publicly available openneuro database.

REFERENCES

1 Alshelh Z, Marciszewski KK, Akhter R, Di Pietro F, Mills EP, Vickers ER, et al. (2018). Disruption of default mode network dynamics in acute and chronic pain states. *NeuroImage Clin.* **17**: 222–231.
2 Baliki MN, Geha PY, Apkarian AV, Chialvo DR (2008). Beyond feeling: chronic pain hurts the brain, disrupting the default-mode network dynamics. *J Neurosci.* **28**: 1398–1403.
3 Baliki MN, Mansour AR, Baria AT, Apkarian AV (2014). Functional reorganization of the default mode network across chronic pain conditions. *PLoS One.* **9**: e106133.
4 Brodersen KH, Wiech K, Lomakina EI, Lin CS, Buhmann JM, Bingel U, et al. (2012). Decoding the perception of pain from fMRI using multivariate pattern analysis. *Neuroimage.* **63**: 1162–1170.
5 Bullmore E & Sporns O (2009). Complex brain networks: graph theoretical analysis of structural and functional systems. *Nat Rev Neurosci.* **10**: 186–198.

6 Čeko M, Frangos E, Gracely J, Richards E, Wang B, Schweinhardt P, et al. (2020). Default mode network changes in fibromyalgia patients are largely dependent on current clinical pain. *Neuroimage.* **216**: 116877.
7 Concina G, Renna A, Grosso A, Sacchetti B (2019). The auditory cortex and the emotional valence of sounds. *Neurosci Biobehav Rev.* **98**: 256–264.
8 Cottam WJ, Iwabuchi SJ, Drabek MM, Reckziegel D, Auer DP (2018). Altered connectivity of the right anterior insula drives the pain connectome changes in chronic knee osteoarthritis. *Pain.* **159**: 929–938.
9 Da Costa S, van der Zwaag W, Marques JP, Frackowiak RS, Clarke S, Saenz M (2011). Human primary auditory cortex follows the shape of Heschl's gyrus. *J Neurosci.* **31**: 14067–14075.
10 Edwards RR, Dworkin RH, Turk DC, Angst MS, Dionne R, Freeman R, et al. (2016). Patient phenotyping in clinical trials of chronic pain treatments: IMMPACT recommendations. *Pain.* **157**: 1851–1871.
11 Elzahaf RA, Tashani OA, Unsworth BA, Johnson MI (2012). The prevalence of chronic pain with an analysis of countries with a Human Development Index less than 0.9: a systematic review without meta-analysis. *Curr Med Res Opin.* **28**: 1221–1229.
12 Felson DT (2009). Developments in the clinical understanding of osteoarthritis. *Arthritis Res Ther.* **11**: 1–11.
13 Galer BS & Jensen MP (1997). Development and preliminary validation of a pain measure specific to neuropathic pain: the Neuropathic Pain Scale. *Neurology.* **48**: 332–338.
14 Hemington KS, Wu Q, Kucyi A, Inman RD, Davis KD (2016). Abnormal cross-network functional connectivity in chronic pain and its association with clinical symptoms. *Brain Struct Funct.* **221**: 4203–4219.
15 Jackson T, Thomas S, Stabile V, Shotwell M, Han X, McQueen K (2016). A systematic review and meta-analysis of the global burden of chronic pain without clear etiology in low-and middle-income countries: trends in heterogeneous data and a proposal for new assessment methods. *Anesth Analg.* **123**: 739–748.
16 Ji J, He Y, Liu L, Xie L (2020). Brain connectivity alteration detection via matrix-variate differential network model. *Biometrics.* **77**: 1409–1421.
17 Kucyi A, Moayedi M, Weissman-Fogel I, Goldberg MB, Freeman BV, Tenenbaum HC, et al. (2014). Enhanced medial prefrontal-default mode network functional connectivity in chronic pain and its association with pain rumination. *J Neurosci.* **34**: 3969–3975.
18 Lambova SN & Müller-Ladner U (2018). Osteoarthritis-current insights in pathogenesis, diagnosis and treatment. *Curr Rheumatol Rev.* **14**: 91–97.
19 Lan F, Lin G, Cao G, Li Z, Ma D, Liu F, et al. (2020). Altered intrinsic brain activity and functional connectivity before and after knee arthroplasty in the elderly: a resting-state fMRI study. *Front Neurol.* **11**: 1087.
20 Lespasio MJ, Piuzzi NS, Husni ME, Muschler GF, Guarino A, Mont MA (2017). Knee osteoarthritis: a primer. *Perm J.* **21**: 16–22.
21 Loggia ML, Kim J, Gollub RL, Vangel MG, Kirsch I, Kong J, et al. (2013). Default mode network connectivity encodes clinical pain: an arterial spin labeling study. *Pain.* **154**: 24–33.
22 Lu M, Su Y, Zhang Y, Zhang Z, Wang W, He Z, et al. (2015). Effectiveness of aquatic exercise for treatment of knee osteoarthritis. *Z Rheumatol.* **74**: 543–552.
23 Michael JW-P, Schlüter-Brust KU, Eysel P (2010). The epidemiology, etiology, diagnosis, and treatment of osteoarthritis of the knee. *Dtsch Arztebl Int.* **107**: 152–162.
24 Napadow V, LaCount L, Park K, As-Sanie S, Clauw DJ, Harris RE (2010). Intrinsic brain connectivity in fibromyalgia is associated with chronic pain intensity. *Arthritis Rheum.* **62**: 2545–2555.
25 Onitsuka T, Shenton ME, Salisbury DF, Dickey CC, Kasai K, Toner SK, et al. (2004). Middle and inferior temporal gyrus gray matter volume abnormalities in chronic schizophrenia: an MRI study. *Am J Psychiatry.* **161**: 1603–1611.
26 Sá KN, Moreira L, Baptista AF, Yeng LT, Teixeira MJ, Galhardoni R, et al. (2019). Prevalence of chronic pain in developing countries: systematic review and meta-analysis. *Pain Rep.* **4**: e779.
27 Schaible H-G (2012). Mechanisms of chronic pain in osteoarthritis. *Curr Rheumatol Rep.* **14**: 549–556.
28 Selvarajah D, Awadh M, Gandhi R, Wilkinson ID, Tesfaye S (2018). Alterations in somatomotor network functional connectivity in painful diabetic neuropathy—a resting state functional magnetic resonance imaging study. *Diabetes.* **67**(Supplement_1): 61–OR.
29 Smith SM, Miller KL, Salimi-Khorshidi G, Webster M, Beckmann CF, Nichols TE, et al. (2011). Network modelling methods for FMRI. *Neuroimage.* **54**: 875–891.
30 Sporns O, Tononi G, Edelman GM (2000). Theoretical neuroanatomy: relating anatomical and functional connectivity in graphs and cortical connection matrices. *Cerebral Cortex.* **10**: 127–141.
31 Tanasescu R, Cottam WJ, Condon L, Tench CR, Auer DP (2016). Functional reorganisation in chronic pain and neural correlates of pain sensitisation: a coordinate based meta-analysis of 266 cutaneous pain fMRI studies. *Neurosci Biobehav Rev.* **68**: 120–133.
32 Taylor AM, Harris AD, Varnava A, Phillips R, Hughes O, Wilkes AR, et al. (2016). Neural responses to a modified Stroop paradigm in patients with complex chronic musculoskeletal pain compared to matched controls: an experimental functional magnetic resonance imaging study. *BMC Psychol.* **4**: 5.
33 Timmers I, López-Solà M, Heathcote LC, Heirich M, Rush GQ, Shear D, et al. (2021). Amygdala functional connectivity mediates the association between catastrophizing and threat-safety learning in youth with chronic pain. *Pain.* Epub ahead of print.
34 Tzourio-Mazoyer N, Landeau B, Papathanassiou D, Crivello F, Etard O, Delcroix N, et al. (2002). Automated anatomical labeling of activations in SPM using a macroscopic anatomical parcellation of the MNI MRI single-subject brain. *Neuroimage.* **15**: 273–289.
35 Weinberger NM (2015). New perspectives on the auditory cortex: learning and memory. *Handb Clin Neurol.* **129**: 117–147.
36 Zalesky A, Fornito A, Bullmore ET (2010). Network-based statistic: identifying differences in brain networks. *Neuroimage.* **53**: 1197–1207.

Appendix A. Target Anatomical Areas according to the AAL Atlas

Index	Regions	Abbr.	Index	Regions	Abbr.
1	Precentral_L	PreCG.L	36	Hippocampus_R	HIP.R
2	Precentral_R	PreCG.R	37	ParaHippocampal_L	PHG.L
3	Frontal_Sup_L	SFGdor.L	38	ParaHippocampal_R	PHG.R
4	Frontal_Sup_R	SFGdor.R	39	Amygdala_L	AMYG.L
5	Frontal_Sup_Orb_L	ORBsup.L	40	Amygdala_R	AMYG.R
6	Frontal_Sup_Orb_R	ORBsup.R	41	Calcarine_L	CAL.L
7	Frontal_Mid_L	MFG.L	42	Calcarine_R	CAL.R
8	Frontal_Mid_R	MFG.R	43	Lingual_L	LING.L
9	Frontal_Mid_Orb_L	ORBmid.L	44	Lingual_R	LING.R
10	Frontal_Mid_Orb_R	ORBmid.R	45	Fusiform_L	FFG.L
11	Frontal_Inf_Oper_L	IFGoperc.L	46	Fusiform_R	FFG.R
12	Frontal_Inf_Oper_R	IFGoperc.R	47	Postcentral_L	PoCG.L
13	Frontal_Inf_Tri_L	IFGtriang.L	48	Postcentral_R	PoCG.R
14	Frontal_Inf_Tri_R	IFGtriang.R	49	Parietal_Inf_L	IPL.L
15	Frontal_Inf_Orb_L	ORBinf.L	50	SupraMarginal_L	SMG.L
16	Frontal_Inf_Orb_R	ORBinf.R	51	SupraMarginal_R	SMG.R
17	Rolandic_Oper_L	ROL.L	52	Precuneus_L	PCUN.L
18	Rolandic_Oper_R	ROL.R	53	Precuneus_R	PCUN.R
19	Supp_Motor_Area_L	SMA.L	54	Caudate_L	CAU.L
20	Supp_Motor_Area_R	SMA.R	55	Caudate_R	CAU.R
21	Olfactory_L	OLF.L	56	Putamen_L	PUT.L
22	Olfactory_R	OLF.R	57	Putamen_R	PUT.R
23	Frontal_Sup_Medial_L	SFGmed.L	58	Pallidum_L	PAL.L
24	Frontal_Sup_Medial_R	SFGmed.R	59	Pallidum_R	PAL.R
25	Frontal_Mid_Orb_L	ORBsupmed.L	60	Thalamus_L	THA.L
26	Frontal_Mid_Orb_R	ORBsupmed.R	61	Thalamus_R	THA.R
27	Insula_L	INS.L	62	Heschl_L	HES.L
28	Insula_R	INS.R	63	Heschl_R	HES.R
29	Cingulum_Ant_L	ACG.L	64	Temporal_Sup_L	STG.L
30	Cingulum_Ant_R	ACG.R	65	Temporal_Sup_R	STG.R
31	Cingulum_Mid_L	DCG.L	66	Temporal_Pole_Sup_L	TPOsup.L
32	Cingulum_Mid_R	DCG.R	67	Temporal_Pole_Sup_R	TPOsup.R
33	Cingulum_Post_L	PCG.L	68	Temporal_Mid_L	MTG.L
34	Cingulum_Post_R	PCG.R	69	Temporal_Mid_R	MTG.R
35	Hippocampus_L	HIP.L	70	Temporal_Inf_L	ITG.L

Abbr: abbreviations. L and R correspond to left (L) and right